

CONTROL OF A TARGET TRACKING SYSTEM EMBEDDED IN A MOVING BODY

Maurício Gruzman, maurgruzman@hotmail.com

Hans Ingo Weber, hans@puc-rio.br

Pontifícia Universidade Católica do Rio de Janeiro. R. Marquês de São Vicente 225, Rio de Janeiro, RJ, CEP 22453-900, Brazil

Luciano Luporini Menegaldo, lmeneg@ime.eb.br

Instituto Militar de Engenharia. Praça Gen Tibúrcio 80, Praia Vermelha, Rio de Janeiro, RJ, CEP 22290-270, Brazil

***Abstract.** This paper presents a control approach for a target tracking system embedded in a moving body. The system comprises a Cardan suspension with dry and viscous friction, sensors, and two permanent magnet DC motors, connected to each of the suspension axis. The motors are controlled by the armature voltage, with saturation limits. Three sensors assembled in the inner link of the suspension are used, one vision sensor and two rate gyros. The vision sensor provides the angular errors of azimuth and elevation of the target with respect to the axial axis. The rate gyros provide the absolute angular speed of the inner link in two orthogonal directions to the axial axis of the vision sensor. An encoder is also used to measure the relative angle between the suspension links. Independent controllers with two feedback loops are used for each motor. The output of the external loop is an increment (or decrement) for the desired absolute angular speed. This loop is slower than the internal loop due to the larger update period of data from the vision sensor. The increment (or decrement) for the desired absolute angular speed is obtained by a fuzzy logic controller. Targets angular errors with respect to the axial axis and the value of the voltage provided to the DC motor are the inputs for this controller. The voltage is also used as an input in order to avoid an increase in the desired absolute angular speed if the control signal provided to the motor (voltage) is already saturated. The inner loop consists of a PI controller with anti-windup action, whose objective is to maintain the absolute angular speed into the desired value. The input for the PI controller is the absolute angular speed error, consisting in the desired absolute angular speed minus the absolute angular speed measured by the rate gyro. The output is the voltage for the DC motor. Results of numerical simulations with a sophisticated model of the system (with no linearization of the equations, dry and viscous friction torques, time delays in control and armature current limiters) supports the effectiveness of the control approach proposed in this work.*

***Keywords:** fuzzy logic control, PI control, target tracking system, systems with time delay*

1. INTRODUCTION

In many military and civilian applications we can find equipments assembled into moving bodies, which must point to a target. They need to be isolated from the rotational motion of the body where they are mounted (called body 0 in this work). This can be achieved with a system composed by a Cardan suspension (introducing therefore bodies 1 and 2), two motors connected to each axis and two rate gyros mounted in body 2 to measure the angular absolute speeds in two directions perpendicular to the axial axis, as presented in Fig. 1. With the information provided by the rate gyros a controller commands the motors in order to compensate any perturbation that is transmitted to body 2. At the same time, the equipment must also follow a target. Therefore a vision sensor can be mounted in body 2 to provide information about targets angular errors with respect to the axial axis. To point precisely to the target the controller should command the motors in order to keep the angular errors equal to zero. Apparently, a contradictory task is sought at the same time: the controller needs to stabilize the equipment with respect to inertial frame, however it must also move the equipment to follow a target. This contradiction is only apparent, since both actions can be combined efficiently in a two loop controller. With information received from the vision sensor, the outer loop calculates the desired absolute angular speeds for body 2, in order to point to the target. The inner loop pursues to keep body 2 absolute angular speeds in the desired values, by comparing the information from the outer loop and the rate gyros. This approach has been discussed by (Brdys and Littler, 2002), (Masten, 2008) and (Kennedy and Kennedy, 2003).

In this work, all bodies are rigid, there is no backlash in gear reduction, actuators are permanent magnet DC motors controlled by armature voltage, sensor errors and noise are disregarded and the motion of body 0 is prescribed. Control signals (voltages) saturation and armature current limiters are considered.

Many authors model pointing/target tracking systems in frequency domain, this may often result in excessive simplification of the dynamic equations that are usually highly non-linear. In this work the differential equations that represent the system are integrated with respect to time. This avoids the need of linearization. Besides, adequate dry friction torque models and controllers with inner and outer loops, having different time delays, can be included with no further difficulties. The main contribution of this work is the presentation of an efficient control approach for target tracking systems embedded in moving bodies, tested in simulations where a sophisticated model of the system is used.

2. EQUATIONS OF MOTION OF THE DEVICE

The equations of motion of the device can be obtained by Lagrange formulation. It is not the aim of this work to study the dynamics of the body 0, therefore it is assumed that its motion is prescribed. The position vector of its center of mass (point a in Fig. 1) with respect to the inertial frame origin will be called ${}^0\mathbf{d}_a$. The position vectors of body 1 and 2 centers of mass, with respect to the center of the Cardan suspension (point b), are respectively ${}^b\mathbf{d}_c$ and ${}^b\mathbf{d}_d$. The orientation coordinates of body 0 can be given by the angles of successive rotations called pitch (δ), yaw (ψ) and roll (γ), presented in Fig. 2.

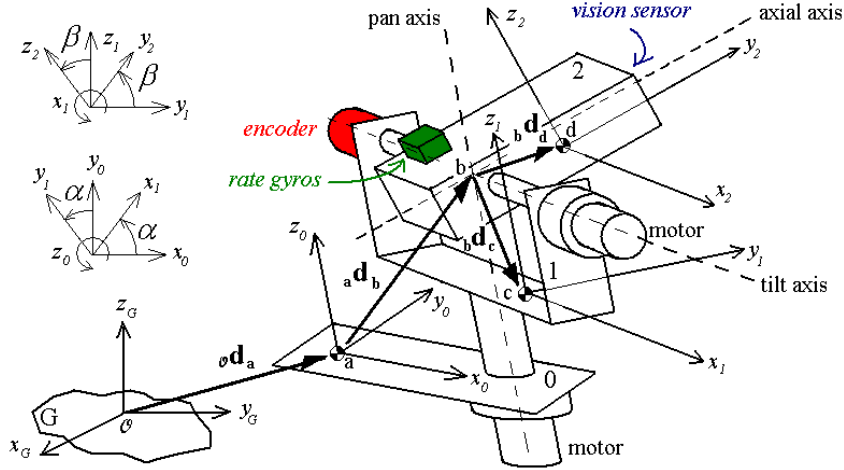


Figure 1. Device, composed by bodies 1 e 2, assembled in a moving body

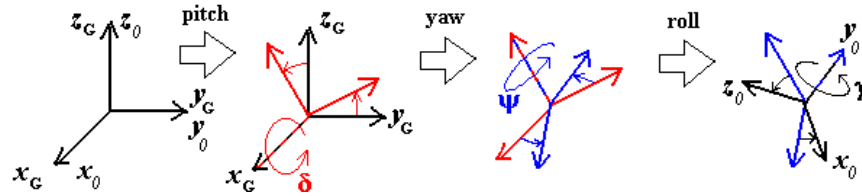


Figure 2. Orientation coordinates of body 0 with respect to inertial frame (G)

It can be seen in Fig. 1 that center-of-mass fixed reference frames are used. They are chosen in such a way that z_0 and z_1 remain parallel to the pan axis, x_1 and x_2 to the tilt axis and y_2 to the axial axis. The angle α corresponds to the rotation angle of body 1 (external link of the suspension) relative to body 0 measured around the pan axis. The angle β corresponds to the rotation angle of body 2 (comprising the internal link and the equipment that must be pointed to the target) relative to body 1 measured around the tilt axis.

The device has two generalized coordinates (relative angles α and β). Writing the Lagrange equations for the device:

$$\frac{d}{dt} \left(\frac{\partial L}{\partial \dot{\alpha}} \right) - \frac{\partial L}{\partial \alpha} = \xi_\alpha \quad \text{and} \quad \frac{d}{dt} \left(\frac{\partial L}{\partial \dot{\beta}} \right) - \frac{\partial L}{\partial \beta} = \xi_\beta \quad (1)$$

The system's Lagrangian is given by the sum of bodies 1 and 2 Lagrangians, each containing the potential and kinetic energy of the bodies. These terms are calculated in (Gruzman *et al.*, 2009). The term on the right of equations 1 and 2 corresponds to non conservative generalized torques. They include the viscous and dry friction torques (T_{vf} and T_{df}) and the torques (T_m) that will appear because of the motors connected to the rotation axes of the system (except dry friction torques in motor that are included in T_{df}).

$$\xi_\alpha = T_{vf,\alpha} + T_{df,\alpha} + T_{m,\alpha} \quad \text{and} \quad \xi_\beta = T_{vf,\beta} + T_{df,\beta} + T_{m,\beta} \quad (2)$$

The viscous friction torques at the pan and tilt axes are given by (c_α and c_β are the viscous friction coefficients):

$$T_{vf,\alpha} = -c_\alpha \cdot \dot{\alpha} \quad \text{and} \quad T_{vf,\beta} = -c_\beta \cdot \dot{\beta} \quad (3)$$

2.1. Torques due to the motors

Applying Kirchoff's law, the differential equation of the motor armature current i is given by:

$$u = R \cdot i + l \cdot \frac{di}{dt} + k_b \cdot \varpi \quad \longrightarrow \quad \frac{di}{dt} = \frac{u - R \cdot i - k_b \cdot \varpi}{l} \quad (4)$$

where R , l , k_b and ϖ are, respectively, the armature resistance, armature inductance, back-emf constant and the angular velocity of the rotor relative to the motor frame.

The angular moment equation for the motors rotor is:

$$J \dot{\varpi} = k_m \cdot i - t_d - c \cdot \varpi \quad (5)$$

The term $k_b \cdot \varpi$ is the counter electromotive force, $k_m \cdot i$ the torque produced by the motor, J the rotor axial moment of inertia and c the viscous friction coefficient in rotor. If backlash in gear reduction is disregarded, the disturbance torque term at the rotor (t_d) equals T_m divided by the gear reduction ratio (n):

$$t_d = \frac{T_m}{n} \quad (6)$$

ϖ and $\dot{\varpi}$ are related to $\dot{\alpha}$ and $\ddot{\alpha}$ through the following equations:

$$\varpi = n \cdot \dot{\alpha} \quad (7)$$

$$\dot{\varpi} = n \cdot \ddot{\alpha} \quad (8)$$

Substituting equations (7), (8) and (6) in (4) and (5), and using the index p for the parameters of the motor connected to the pan axis:

$$\frac{di_p}{dt} = \frac{u_p - R_p \cdot i_p - k_{b,p} \cdot n_p \cdot \dot{\alpha}}{l_p} \quad (9)$$

$$J_p \cdot n_p \cdot \ddot{\alpha} = k_{m,p} \cdot i_p - \frac{T_{m,\alpha}}{n_p} - c_p \cdot n_p \cdot \dot{\alpha} \quad (10)$$

Equation (10) can be solved for $T_{m,\alpha}$:

$$T_{m,\alpha} = n_p \cdot k_{m,p} \cdot i_p - c_p \cdot n_p^2 \cdot \dot{\alpha} - J_p \cdot n_p^2 \cdot \ddot{\alpha} \quad (11)$$

By a similar way, it can be found for the tilt axis and the corresponding motors armature current:

$$\frac{di_t}{dt} = \frac{u_t - R_t \cdot i_t - k_{b,t} \cdot n_t \cdot \dot{\beta}}{l_t} \quad (12)$$

$$T_{m,\beta} = n_t \cdot k_{m,t} \cdot i_t - c_t \cdot n_t^2 \cdot \dot{\beta} - J_t \cdot n_t^2 \cdot \ddot{\beta} \quad (13)$$

Armature current limiters are usually employed to avoid injuries to the motors and circuits. They keep the current between a maximum value (i_{max}) and a minimum value (i_{min}). If the system has limiters, then the first derivative of the currents with respect to time, given by the equations (9) and (12), are set to zero whenever:

$$(i_p \geq i_{max,p}) \text{ and } \left(\frac{u_p - k_{b,p} \cdot n_p \cdot \dot{\alpha}}{R_p} \geq i_{max,p} \right), \quad \text{or,} \quad (i_p \leq i_{min,p}) \text{ and } \left(\frac{u_p - k_{b,p} \cdot n_p \cdot \dot{\alpha}}{R_p} \leq i_{min,p} \right) \quad (14)$$

$$(i_t \geq i_{\max,t}) \text{ and } \left(\frac{u_t - k_{b,t} \cdot n_t \cdot \dot{\beta}}{R_t} \geq i_{\max,t} \right), \quad \text{or,} \quad (i_t \leq i_{\min,t}) \text{ and } \left(\frac{u_t - k_{b,t} \cdot n_t \cdot \dot{\beta}}{R_t} \leq i_{\min,t} \right) \quad (15)$$

2.2. Torques due to dry friction

Dry friction torques are found in the axes, caused mainly by the motor brushes and gear reduction. Dry friction torques at the bearings will be disregarded. The procedure presented in (Piedbceuf and Carufel, 2000) will be used to calculate the dry friction torques at each axis. With this approach the only parameters that need to be known are the dynamic dry friction torque (T_{din}) and the maximum value of the static dry friction torque (T_{limit}) at each axis, which can be obtained with simple experiments.

The dynamic equation of the system, in a matricial form, is given by Eq. (16), where $J_{\alpha,\alpha}$, $J_{\alpha,\beta}$, $J_{\beta,\beta}$, f_1 and f_2 are nonlinear terms.

$$\begin{bmatrix} J_{\alpha,\alpha} & J_{\alpha,\beta} \\ J_{\alpha,\beta} & J_{\beta,\beta} \end{bmatrix} \begin{bmatrix} \ddot{\alpha} \\ \ddot{\beta} \end{bmatrix} + \begin{bmatrix} f_1 \\ f_2 \end{bmatrix} = \begin{bmatrix} T_{df,\alpha} \\ T_{df,\beta} \end{bmatrix} + \begin{bmatrix} T_{vf,\alpha} \\ T_{vf,\beta} \end{bmatrix} + \begin{bmatrix} T_{m,\alpha} \\ T_{m,\beta} \end{bmatrix} \quad (16)$$

In the following we will concentrate our analysis in the generalized coordinate α . The extension to β is straightforward.

If $\dot{\alpha}$ is not zero, it means that body 1 is in slip regime, and the generalized dry friction torque at this body will be:

$$T_{df,\alpha} = -T_{din,\alpha} \cdot \text{sign}(\dot{\alpha}) \quad (17)$$

If $\dot{\alpha} = 0$ and the modulus of the sum of all torques ($T_{TEST,\alpha}$) including torques due to inertia but excluding dry friction torque, is lower than $T_{limit,\alpha}$ it means that body 1 is at the stick regime, and the dry friction torque should be calculated according to Eq. (18).

$$T_{df,\alpha} = -T_{TEST,\alpha} \quad \text{when} \quad -T_{limit,\alpha} < T_{TEST,\alpha} < T_{limit,\alpha} \quad (18)$$

It should be stressed that it is not convenient to consider $\dot{\alpha} = 0$ as a transition condition between stick and slip, since during the numerical resolution of the equations of motion the true zero is not achieved. Besides, it can be observed in experiments that sliding abruptly stops under a minimum angular velocity (v_{min}). Therefore it will be considered that the body is in stick regime whenever the modulus of $\dot{\alpha}$ is lower than $v_{min,\alpha}$ and the modulus of $T_{TEST,\alpha}$ is lower than $T_{limit,\alpha}$. Next, a numerical damping term must be included to the static dry friction torque in order to eliminate the residual angular relative velocity of the body, as it will be seen in the following example.

Considering that at a certain instant during the numerical resolution of the equation system (16), the modulus of $\dot{\alpha}$ is smaller than $v_{lim,\alpha}$ (assuming that the first derivative $\dot{\beta}$ is larger than $v_{lim,\beta}$). Then it must be verified if the modulus of $T_{TEST,\alpha}$ (obtained from the system of equations bellow) is higher or lower than $T_{limit,\alpha}$.

$$\begin{bmatrix} 1 & J_{\alpha,\beta} \\ 0 & J_{\beta,\beta} \end{bmatrix} \begin{bmatrix} T_{TEST,\alpha} \\ \dot{\beta} \end{bmatrix} + \begin{bmatrix} f_1 \\ f_2 \end{bmatrix} = \begin{bmatrix} 0 \\ -T_{din,\beta} \cdot \text{sign}(\dot{\beta}) \end{bmatrix} + \begin{bmatrix} T_{vf,\alpha} \\ T_{vf,\beta} \end{bmatrix} + \begin{bmatrix} T_{m,\alpha} \\ T_{m,\beta} \end{bmatrix} \quad (19)$$

If $|T_{TEST,\alpha}| > T_{limit,\alpha}$ then body 1 is in slip regime and $\ddot{\alpha}$ and $\ddot{\beta}$ are obtained with equation (20):

$$\begin{bmatrix} \ddot{\alpha} \\ \ddot{\beta} \end{bmatrix} = \begin{bmatrix} J_{\alpha,\alpha} & J_{\alpha,\beta} \\ J_{\alpha,\beta} & J_{\beta,\beta} \end{bmatrix}^{-1} \left(\begin{bmatrix} -T_{din,\alpha} \cdot \text{sign}(\dot{\alpha}) \\ -T_{din,\beta} \cdot \text{sign}(\dot{\beta}) \end{bmatrix} + \begin{bmatrix} T_{vf,\alpha} \\ T_{vf,\beta} \end{bmatrix} + \begin{bmatrix} T_{m,\alpha} \\ T_{m,\beta} \end{bmatrix} - \begin{bmatrix} f_1 \\ f_2 \end{bmatrix} \right) \quad (20)$$

otherwise Eq. (21) should be used:

$$\begin{bmatrix} \ddot{\alpha} \\ \ddot{\beta} \end{bmatrix} = \begin{bmatrix} J_{\alpha,\alpha} & J_{\alpha,\beta} \\ J_{\alpha,\beta} & J_{\beta,\beta} \end{bmatrix}^{-1} \left(\begin{bmatrix} -T_{TEST,\alpha} - b_{numeric,\alpha} \cdot \dot{\alpha} \\ -T_{din,\beta} \cdot \text{sign}(\dot{\beta}) \end{bmatrix} + \begin{bmatrix} T_{vf,\alpha} \\ T_{vf,\beta} \end{bmatrix} + \begin{bmatrix} T_{m,\alpha} \\ T_{m,\beta} \end{bmatrix} - \begin{bmatrix} f_1 \\ f_2 \end{bmatrix} \right) \quad (21)$$

As previously discussed, a numerical damping term should be added to dry friction static torque because body 1 is in stick regime. An expression proposed in (Piedbceuf and Carufel, 2000) for the numerical damping coefficient is:

$$b_{numeric,\alpha} = \frac{\eta_\alpha}{v_{lim,\alpha}} \cdot T_{est,\alpha} \quad (22)$$

where η_α is a constant and should be chosen in order to have $J_{\alpha,\alpha}/b_{numeric,\alpha}$ reasonably larger than the minimum integration step of the algorithm used for the resolution of the ordinary differential equations (ODE). In the example presented, stiction occurred only in α , but the method can also be used for stiction in α and β or only in β . It should be stressed that when equation (19) is used for the verification of stiction in a generalized coordinate i (in a system with n generalized coordinates) the following rule should be applied:

$$if \begin{cases} j \neq i \Rightarrow J_{j,i} = 0 \text{ and } T_{df,i} = 0 \\ j = i \Rightarrow J_{j,i} = 1 \end{cases}, \text{ for } j = 1, \dots, n \quad (23)$$

3. RESOLUTION OF THE EQUATIONS CONSIDERING CONTROL SIGNAL TIME DELAY

The resultant system has two first-order ODE, given by equations (9) and (12), and two second-order ODE, given by Eq. (16). The dry friction torques are obtained before each integration step. To obtain only first order ODE the following coordinate transformation can be applied:

$q_1 = \alpha$, $q_2 = \beta$, $q_3 = \dot{\alpha}$, $q_4 = \dot{\beta}$ and the system of equations becomes:

$$\frac{di_p}{dt} = \frac{u_p - R_p \cdot i_p - k_{b,p} \cdot n_p \cdot q_3}{l_p} \quad (24)$$

$$\frac{di_t}{dt} = \frac{u_t - R_t \cdot i_t - k_{b,t} \cdot n_t \cdot q_4}{l_t} \quad (25)$$

$$\dot{q}_1 = q_3 \quad (26)$$

$$\dot{q}_2 = q_4 \quad (27)$$

$$\begin{bmatrix} J_{q_1,q_1} & J_{q_1,q_2} \\ J_{q_1,q_2} & J_{q_2,q_2} \end{bmatrix} \begin{bmatrix} \dot{q}_3 \\ \dot{q}_4 \end{bmatrix} + \begin{bmatrix} f_1 \\ f_2 \end{bmatrix} = \begin{bmatrix} T_{df,q_1} \\ T_{df,q_2} \end{bmatrix} + \begin{bmatrix} T_{vf,q_1} \\ T_{vf,q_2} \end{bmatrix} + \begin{bmatrix} T_{m,q_1} \\ T_{m,q_2} \end{bmatrix} \quad (28)$$

With the initial conditions $q_1(0)$, $q_2(0)$, $q_3(0)$, $q_4(0)$, $i_p(0)$, $i_t(0)$ and the prescribed motion of the body 0, a numerical algorithm for calculation of the approximate solution of first order differential equations system can be used. The voltages provided to the motors (u_p and u_t) are the control variables and are updated during the numerical integration of the whole ODE system at each time interval Δt (corresponds to the time delay that would occur in a real system due to data acquisition by the sensors, data processing and calculation of the control tensions), in the following way:

- i) at the initial instant ($t = 0$) all the tensions are set to zero;
- ii) with data provided by the sensors, at $t = 0$ the control tensions are calculated;
- iii) the ODEs are integrated from $t = 0$, considering constant voltages with the values mentioned in step i);
- iv) when $t = \Delta t$, the integration process stops and, with data from the sensors, new tensions are calculated;
- v) the integration process continues from $t = \Delta t$, considering constant voltages with the values mentioned in step ii);
- vi) when $t = 2\Delta t$, the integration process is interrupted again and, with data from the sensors, new tensions are calculated;
- vii) the integration process starts again from $t = 2\Delta t$, considering constant voltages with the values mentioned in step iv);
- viii) the process is repeated, interrupting the integration at every Δt , until the final simulation time is reached.

4. CONTROL SIGNALS

The controllers need to provide the adequate voltages to the motors in order to keep the axial axis pointed to the target. This means that the angular errors of azimuth (\hat{e}_{az}) and elevation (\hat{e}_{el}) with respect to the axial axis should be kept as near as zero as possible. It is assumed that the vision sensor is mounted adequately at the suspension with its optical axis aligned with the axial axis and such that the errors can be measured from the center of the suspension (point b) that belongs to the axial axis, as drawn in Fig. 3.

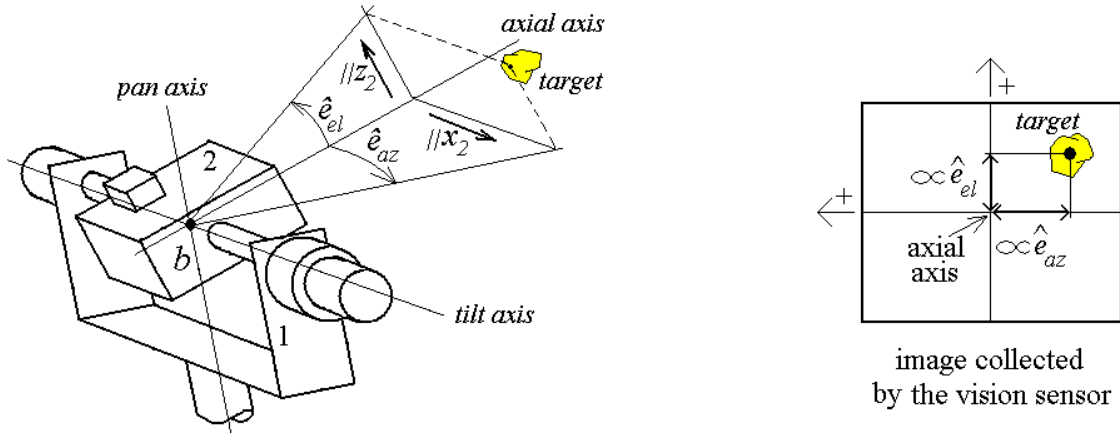


Figure 3. Angular errors of azimuth and elevation with respect to the center of the Cardan suspension

The vision sensor provides the target centroid coordinates in the image plane. These coordinates with respect to the image plane center are proportional to \hat{e}_{az} and \hat{e}_{el} . The time to process the image and calculate the coordinates is usually larger than the control signal update period Δt . As the controller must also provide compensation to body 0 angular motion, a control strategy where the voltages provided to the motors can be updated faster than the information from vision sensor is necessary. A method that is commonly used and discussed in (Brdys and Littler, 2002), (Masten, 2008) and (Kennedy and Kennedy, 2003) consists in the use of independent controllers for each motor, with an external loop (also called tracking loop) and an internal loop (also called stabilization loop). One of the controllers has the objective to keep body 2 absolute angular speed in x_2 direction at some desired value. The other one, to keep body 2 absolute angular speed in z_2 direction at some desired value. With information about the angular errors, the desired values are calculated at the external loops. In the inner loop, working in a higher sampling frequency, the voltage provided to the motor in order to keep the absolute angular speed in x_2 direction (or z_2) at the desired value is calculated and updated at every time interval Δt . The input for this loop is an error signal equal to the desired absolute angular speed minus the value measured by one of the rate gyros mounted in body 2. In the proposed control approach, the internal loops have PI (proportional and integral) controllers with anti-windup (Aström and Murray, 2008) and the outer loops incremental fuzzy logic controllers (FLC). The FLC output is an increment for the desired angular absolute speed for body 2 in x_2 direction (or z_2). The inputs for the FLC are the angular errors provided by the vision sensor, their derivatives with respect to time and a variable called LoSu. This variable corresponds to the saturation level of the control signal, and is used to avoid increments for the desired absolute angular speed if the control signal is near its superior saturation limit (or decrements if it is near the inferior saturation limit). One controller provides the voltage to the tilt motor in order to keep body 2 absolute angular speed in x_2 direction at the desired value. The other controller provides the voltage to the pan motor to keep the angular absolute speed in x_2 direction at the desired value. It is important to remember that the pan motor axis is parallel to z_1 and not z_2 , therefore the error comprising body 2 absolute angular speed in z_2 direction minus the absolute angular velocity in this direction, measured by the rate gyro, should be divided by $\cos\beta$. The relative angle β can be measured by an encoder mounted at the tilt axis (see Fig. 1). If the systems working space is limited to $-90^\circ < \beta < +90^\circ$ there is no risk to have a division by zero. In Fig. 4 the pan motor general control structure is presented. For the tilt motor the structure is similar, but there is no division by $\cos\beta$ at the stabilization loop. The outer loop time delay is $\Delta t'$. The inner loop time delay is Δt and $\Delta t' > \Delta t$.

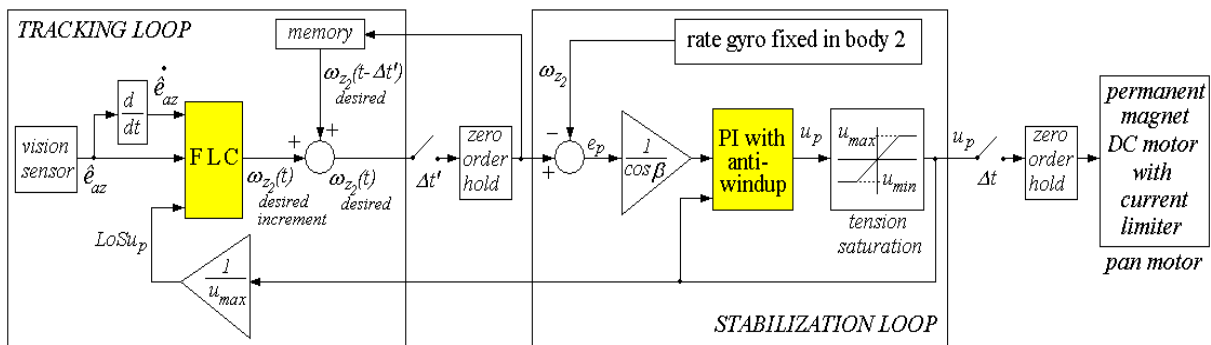


Figure 4. Pan motor general control structure

4.2. Inner loop (stabilization loop)

In the inner loops PI controllers are used. The inputs are the errors comprising the desired absolute angular speeds minus the absolute angular speeds measured with the rate gyros. If digital controllers are used, the control signals provided to the pan and tilt motors are given by the equations bellow:

$$u_p = k_{p,p} \cdot e_p + k_{i,p} \cdot \sum e_p \cdot \Delta t \quad \text{and} \quad u_t = k_{p,t} \cdot e_t + k_{i,t} \cdot \sum e_t \cdot \Delta t \quad (29)$$

where k_p and k_i are the gains of the proportional and integral terms, respectively. The errors are given by:

$$e_p = \frac{\omega_{z_2 \text{ desired}} - \omega_{z_2}}{\cos \beta} \quad \text{and} \quad e_t = \omega_{x_2 \text{ desired}} - \omega_{x_2} \quad (30)$$

where $\omega_{z_2 \text{ desired}}$ and $\omega_{x_2 \text{ desired}}$ are body 2 desired absolute angular speeds in z_2 and x_2 directions. They are updated by the outer loop at every time interval $\Delta t'$. The two rate gyros assembled in body 2 provide new measurements of ω_{z_2} and ω_{x_2} in a faster rate. Therefore the voltages can be updated at every time interval Δt .

If the absolute angular speed takes a long time to reach the desired value, the sum in Eq. (29) may become excessively large and will keep increasing even if the control signal is saturated. The control signal will then remain saturated even when the error changes sign and it may take a long time before the integrator and the controller output come inside saturation range. This problem is called integrator windup and can be avoided if an anti-windup action is included at control. A common anti-windup strategy is the back-calculation (Aström and Murray, 2008) that is efficient but has a gain that needs to be adjusted. Therefore, in this work a simpler method will be used where the sum in Eq. (29) is interrupted if the control signal is at the maximum saturation limit and the error is positive, or, if the control signal is at the minimum saturation limit and the error is negative.

In real applications the system parameters like body inertias, friction coefficients, motors parameters (armature resistance, inductance, torque constant, back-emf constant) and control time delays may be unknown and some heuristic method like Ziegler-Nichols (Aström and Murray, 2008) can be used to tune experimentally the PI gains. In this work, the gains of the inner loop PI controllers will be obtained by the Ziegler-Nichols frequency response method. The method should be performed independently for the controller of each motor and consists of sending a constant reference signal to a proportional controller, as the schematic draw of Fig. 5 shows. Next, the proportional gain is increased until the plant response becomes a sustained oscillation for the first time. This gain is called critical gain (k_{crit}) and the oscillation period is called critical period (T_{crit}). The proportional and integral gains of the PI controller will be given by equations (31) and (32).

$$k_p = 0.45 \cdot k_{crit} \quad (31)$$

$$k_i = \frac{k_p}{0.8 \cdot T_{crit}} \quad (32)$$

To tune the inner loop PI controller a constant desired absolute angular speed is used as the reference signal, as shown in Fig. 5. The rate gyro provides the feedback signal. When tuning the gains for the pan motor controller the systems base and the tilt axis should be kept fixed (the relative angle β can be held fixed at 0° for example). When tuning the gains for the tilt motor controller the systems base and the pan axis should be kept fixed. The Ziegler-Nichols tuning can also be done with simulations instead of experiments, if the system parameters are available for simulation.

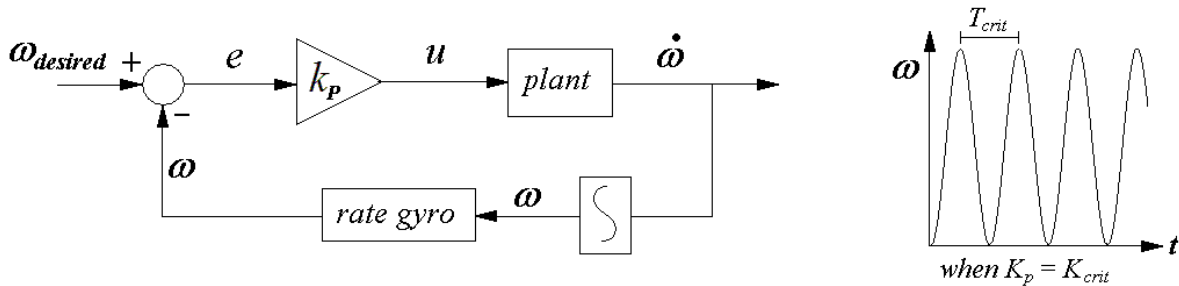


Figure 5. Closed loop system used for Ziegler-Nichols Tuning

4.3. Outer loop (tracking loop)

In the outer loop there is a vision sensor to collect images from the target. The image is processed and the target identified on the image plane. To differentiate the target from the image background some of its characteristic must be previously known, as his color or shape for example. Next, the targets centroid coordinates in the image plane are calculated. Those coordinates are proportional to the elevation and azimuth angular errors, as shown in Fig. 3. Afterwards, each angular error is provided to a Fuzzy Logic Controller (Pasino and Yurkovich, 1998) whose output is an increment to the desired absolute angular speed, used as reference in the inner loop. In this work FLC were chosen for the external loops because they are more flexible then traditional controllers, like PID, due to the possibility of implementing nonlinear mappings between inputs and outputs. It is not the objective of this work to study how the image is processed or how the targets image centroid is calculated. For the model used in this work the only necessary information is the time duration $\Delta t'$ of the whole process that occurs in the tracking loop. This time delay, from the instant when the image is collected until the instant when the desired absolute angular speed is provided to the inner loop, is relatively large when compared with Δt . The biggest part of $\Delta t'$ usually comprises the time that the vision sensor takes to provide the values of the angular errors.

The inputs for the FLC used at the pan motor control are the angular azimuth error (\hat{e}_{az}), the derivative of this error with respect to time and the control voltage saturation level ($LoSu_p$). The $LoSu_p$ is used to avoid increments for the desired absolute angular speeds if the control signal is near its superior saturation limit (or decrements if it is near the inferior limit). The pan motor FLC output is an increment for body 2 desired absolute angular speed in z_2 direction (ω_{z_2} desired increment). This increment is added to the previous value of the referred angular speed (stored in memory) resulting in the value that will be provided to the internal loop (ω_{z_2} desired). The inputs for the tilt motor FLC are the elevation angular error (\hat{e}_{el}), the derivative of this error with respect to time and the control voltage saturation level ($LoSu_t$). The output is an increment for body 2 desired absolute angular speed x_2 direction (ω_{x_2} desired increment). The angular errors derivatives in a certain instant t_k can be approximated according to Eq. (33). The control signal saturation levels are given by Eq. (34), where $u_{SAT,p}$ and $u_{SAT,t}$ are the values of the maximum voltage that can be provided for each motor.

$$\dot{e}_p(t_k) \approx \frac{\hat{e}_p(t_k) - \hat{e}_p(t_k - \Delta t')}{\Delta t'} \quad \text{and} \quad \dot{e}_t(t_k) \approx \frac{\hat{e}_t(t_k) - \hat{e}_t(t_k - \Delta t')}{\Delta t'} \quad (33)$$

$$LoSu_p = \frac{u_p}{u_{SAT,p}} \quad \text{and} \quad LoSu_t = \frac{u_t}{u_{SAT,t}} \quad (34)$$

Both FLC use the input and output membership functions shown in Fig. 6 and the rule-base of Tab. 1. The algorithm used for inference is max-min method and for defuzzification is the center of area method (Pasino and Yurkovich, 1998).

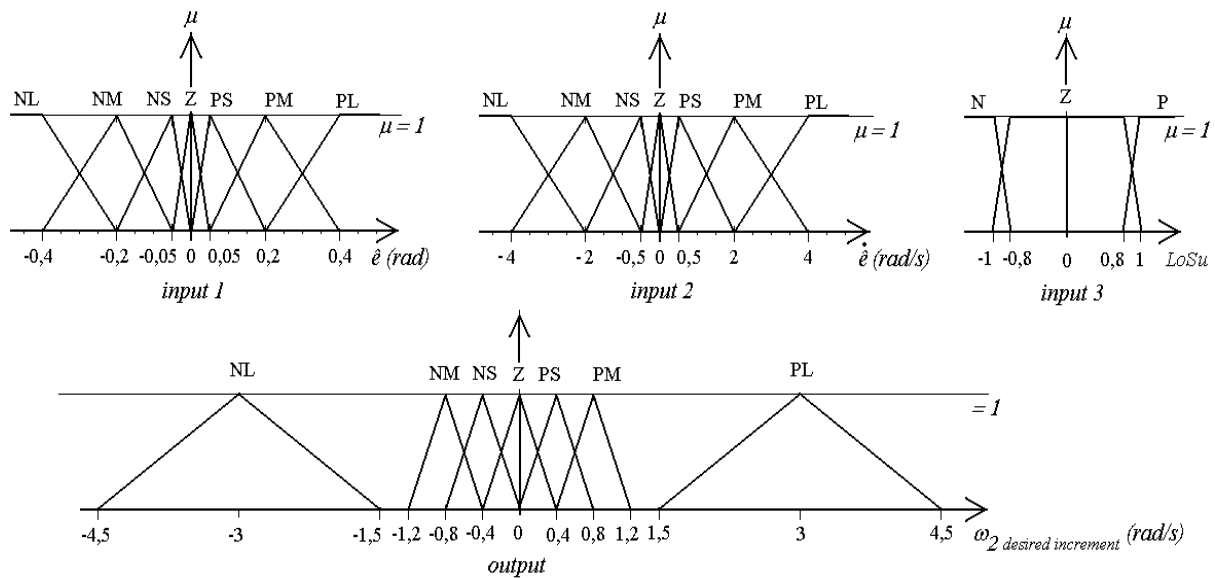


Figure 6. Membership functions for the FLC with three inputs (\hat{e} , $\dot{\hat{e}}$ and $LoSu$) and one output (ω_{z_2} desired increment)

Table 1. Rule-base for the FLC with three inputs (\hat{e} , $\dot{\hat{e}}$ and $LoSu$) and one output (ω_2 desired increment).

		$LoSu = N$						$LoSu = Z$						$LoSu = P$								
		NL	NM	NS	Z	PS	PM	PL	NL	NM	NS	Z	PS	PM	PL	NL	NM	NS	Z	PS	PM	PL
$\dot{\hat{e}}$	\hat{e}	NL	Z	Z	Z	Z	Z	Z	NL	NL	NL	NL	NM	NM	NM	NL	NL	NL	NL	NM	NM	NM
	NM	Z	Z	Z	Z	Z	Z	Z	NL	NL	NL	NM	NM	NS	NS	NL	NL	NL	NM	NM	NS	NS
	NS	Z	Z	Z	Z	Z	Z	Z	NL	NL	NM	NM	NS	Z	Z	NL	NL	NM	NM	NS	Z	Z
	Z	Z	Z	Z	Z	PS	PS	PM	NM	NS	NS	Z	PS	PS	PM	NM	NS	NS	Z	Z	Z	Z
	PS	Z	Z	PS	PM	PM	PL	PL	Z	Z	PS	PM	PM	PL	PL	Z	Z	Z	Z	Z	Z	Z
	PM	PS	PS	PM	PM	PL	PL	PL	PS	PS	PM	PM	PL	PL	PL	Z	Z	Z	Z	Z	Z	Z
	PL	PM	PM	PM	PL	PL	PL	PL	PM	PM	PM	PL	PL	PL	PL	Z	Z	Z	Z	Z	Z	Z

The membership functions and rule-base presented were adjusted through simulations of systems with outer loop time delay ($\Delta t'$) varying between 10ms and 20ms. For $\Delta t'$ out of that range a new adjustment may be necessary. But it is important to emphasize that there is no need for adjustments in the FLC if there are any changes in other system parameters, as inertias, motor parameters, friction coefficients, inner loop time delay (Δt), etc. Changes in those parameters, however, demand a new tuning of the inner loop PI controller gains, as discussed in section 4.2.

5. SIMULATION RESULTS

The following data were used in the first simulation:

Gravity acceleration (g): 9,81 m/s². Body 1 mass (m_1): 0.3 kg. Body 2 mass (m_2): 0.4 kg. Viscous friction coefficients at the axes: $c_\alpha=c_\beta=0.0001$ kg m²/rad s. Motors parameters: $c_p=c_i=0.00005$ kg m²/rad s, $J_p=J_i=0.00003$ kg m², $n_p=n_i=30$, $R_p=R_i=2.3$ Ω , $l_p=l_i=0.003$ H, $k_{m,p}=k_{m,i}=k_{b,p}=k_{b,i}=0,045$ V/rad/s. Dry friction (static and dynamic) torques: $T_{est,\alpha}=T_{est,\beta}=0.5$ Nm and $T_{din,\alpha}=T_{din,\beta}=0.4$ Nm. Maximum and minimum current limits at the motor armatures: $i_{max}=10A$ and $i_{min}=-10A$.

Position vector of the center of the Cardan suspension (point b) with respect to body 0 center of mass (in coordinates of body 0 fixed frame), position vector of body 1 center of mass with respect to point b (in coordinates of body 1 fixed frame) and position vector of body 2 center of mass with respect to point b (in coordinates of body 2 fixed frame) are given respectively by:

$${}^0\mathbf{d}_b = [0 \ 0.5 \ 0]^T \text{ m}, \quad {}^1\mathbf{d}_c = [0 \ 0 \ -0.02]^T \text{ m} \text{ and } {}^2\mathbf{d}_d = [0.01 \ 0.04 \ 0.025]^T \text{ m}.$$

Body 1 and 2 inertia tensors, expressed in coordinates of body 1 and 2 frames, respectively:

$${}^1I_1 = \begin{bmatrix} 2.59 & -0.44 & 0.14 \\ -0.44 & 4.69 & -0.69 \\ 0.14 & -0.69 & 2.72 \end{bmatrix} \cdot 10^{-4} \text{ kg m}^2 \text{ and } {}^2I_2 = \begin{bmatrix} 9.76 & -1.14 & -0.32 \\ -1.14 & 4.67 & -1.51 \\ -0.32 & -1.51 & 9.57 \end{bmatrix} \cdot 10^{-4} \text{ kg m}^2$$

Prescribed motion: body 0 center of mass (point a) position vector with respect to inertial frame origin (O), body 0 orientation angles (δ , ψ and γ) and targets (tt) position vector with respect to O in inertial frame coordinates:

$${}^G\mathbf{d}_a(t) = [\sin(2\pi t) \ 300t \ \sin(3\pi t)]^T \text{ m}, \quad \delta(t)=0.2\sin(6\pi t) \text{ rad}, \quad \psi(t)=0.2\cos(6\pi t) \text{ rad}, \quad \gamma(t)=4\pi t \text{ rad}.$$

$${}^G\mathbf{d}_{tt}(t) = [\cos(3.5\pi t) \ 5 + 300t \ \sin(2.7\pi t)]^T \text{ m}$$

Outer loop time delay ($\Delta t'$): 15 ms. Inner loop time delay (Δt): 1 ms. Maximum control voltages: +24V. Minimum control voltages: - 24V. Inner loop gains obtained with Ziegler-Nichols tuning: $K_{p,p}=K_{p,i}=17.41$, $K_{l,p}=K_{l,i}=2176.88$. The membership functions and rule-base used in the outer loop FLC are defined in section 4.3. Algorithm used for calculating the approximate solution of the ODE: Fourth Order Runge-Kutta.

In the second simulation the same data of simulation 1 were used (including inner loop gains) except the following:

Inner loop time delay(Δt): 1.5 ms. Gear reduction ratio: $n_p=n_i=10$. Dry friction (static and dynamic) torques: $T_{est,\alpha}=T_{est,\beta}=0.17$ Nm and $T_{din,\alpha}=T_{din,\beta}=0.13$ Nm.

$${}^1\mathbf{d}_c = {}^2\mathbf{d}_d = \begin{bmatrix} 0 \\ 0 \\ 0 \end{bmatrix} \text{ m} \quad {}^1I_1 = \begin{bmatrix} 5 & 0 & 0 \\ 0 & 10 & 0 \\ 0 & 0 & 5 \end{bmatrix} \cdot 10^{-4} \text{ kg m}^2, \quad {}^2I_2 = \begin{bmatrix} 6 & 0 & 0 \\ 0 & 3 & 0 \\ 0 & 0 & 6 \end{bmatrix} \cdot 10^{-4} \text{ kg m}^2$$

In the third simulation data of simulation 2 were used, except the inner loop gains, that were tuned again by the Ziegler-Nichols method: $K_{p,p}= 5.22$, $K_{l,p}= 483.3$, $K_{p,i}= 4.59$ and $K_{l,i}= 425$.

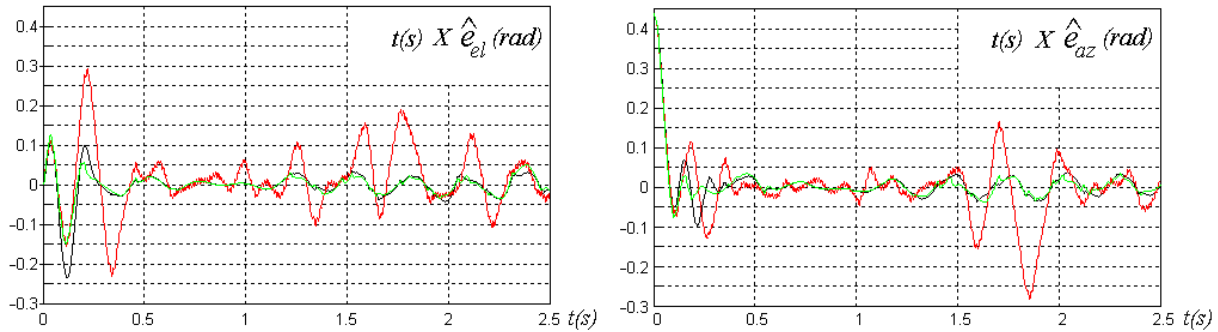


Figure 7. Angular errors of elevation (left) and azimuth (right), in simulation 1 (black), 2 (red) and 3 (green)

In the simulations where the inner loop gains were tuned by Ziegler-Nichols method (black and green graphs) the errors remained under ± 0.05 rad after 0.25s of simulation. The same membership functions and rule-base for the outer loop FLC were used in all simulations.

6. CONCLUSIONS

A control approach for target tracking systems is presented in this work. Independent controllers are used for each motor. Four sensors are employed: one vision sensor, two rate gyros and one encoder (used for the pan motor control only). Since the vision sensor takes a longer time than the other sensors to provide its measurements, it is more efficient to use two loops in each controller. The outer loop, with information from the vision sensor, calculates the desired absolute angular speeds for body 2 with a FLC, in order to point the axial axis to the target. The inner loop, that is faster, uses information from the other sensors in order to keep body 2 angular absolute speeds in the desired values. A PI controller with anti-windup action is used in this loop. To verify the efficiency of the controller, results of simulation are presented. At the simulations the differential equations are integrated with respect to time. Working in time domain instead of frequency domain allows a more realistic representation of the system, since the equations of motion are not linearized. Besides that, dry friction torques and different time delays for the controller loops can be implemented with relative simplicity. Saturation in armature current and control voltages were also considered. In the simulation presented (where body 0 had translational and rotational motion, with relatively large amplitude and frequency) the angular errors remained under ± 0.05 rad when the inner loop gains were tuned by Ziegler-Nichols method. There was no need to adjust the membership functions and rule-base of the outer loop FLC when different system parameters were used. Since there is a FLC in the outer loop and the inner loop has a PI controller whose gains can be adjusted by Ziegler-Nichols method it is possible to implement this control when the system parameters are unknown.

An experimental set-up is being constructed to validate the system with the results achieved.

7. ACKNOWLEDGEMENTS

The authors gratefully acknowledge the support of CNPq.

8. REFERENCES

- Aström, K.J. and Murray, R.M., 2008, "Feedback Systems; An Introduction for Scientists and Engineers", Princeton University Press, New Jersey, USA, 396 p.
- Brdys, M.A., and Littler, J.J., 2002, "Fuzzy Logic Gain Scheduling for Non-Linear Servo Tracking", Int. J. Appl. Math. Comp. Sci., Vol.12, No.2, pp. 209-219.
- Gruzman, M., Weber, H.I. and Menegaldo, L.L., 2009, "Modeling of a Pointing and Target Tracking System", Proceedings of the 13th International Symposium on Dynamic Problems of Mechanics, Angra dos Reis, Brazil.
- Kennedy, P.J. and Kennedy, R.L., 2003, "Direct Versus Indirect Line of Sight (LOS) Stabilization", IEEE transactions on Control Systems Technology, Vol.11, No. 1, pp. 3-15.
- Masten, M. K., 2008, "Inertially Stabilized Platforms for Optical Imaging Systems", IEEE Control Systems Magazine, Vol. 28, No. 1, pp. 47-64.
- Pasino, K.M. and Yurkovich, S., 1998, "Fuzzy Control", Addison-Wesley Longman, California, USA, 502 p.
- Pidbceuf, J.C., and Carufel, J. de., 2000, "Friction and Stick-Slip in Robots: Simulation and Experimentation", Multibody Systems Dynamics, Vol.4, pp. 341-354.

9. RESPONSIBILITY NOTICE

The authors are the only responsible for the printed material included in this paper.